Biogeosciences Discuss., https://doi.org/10.5194/bg-2018-52
Manuscript under review for journal Biogeosciences
Discussion started: 26 February 2018

Southern Ocean controls of the vertical marine $\delta^{13}C$ gradient – a modelling study

Anne L. Morée[1], Jörg Schwinger[2], Christoph Heinze[12]

[1]Geophysical Institute, University of Bergen, Bjerknes Centre for Climate Research, 5007 Bergen, Norway
[2]Uni Research Climate, Bjerknes Centre for Climate Research, 5007 Bergen, Norway

Correspondence to: Anne L. Morée (anne.moree@uib.no)

Abstract. The standardised ^{13}C isotope, $\delta^{13}C$, is a widely used ocean tracer to study changes in ocean circulation, water mass ventilation, atmospheric pCO_2 and the biological carbon pump on timescales ranging from decades to 10s of millions of years. $\delta^{13}C$ data derived from ocean sediment core analysis provide information on $\delta^{13}C$ of dissolved inorganic carbon and the vertical $\delta^{13}C$ gradient (i.e., $\Delta\delta^{13}C$) in past oceans. In order to correctly interpret $\delta^{13}C$ and $\Delta\delta^{13}C$ variations, a good understanding is needed of the influence from ocean circulation, air-sea gas exchange and biological productivity on these variations. The Southern Ocean is a key region for these processes, and we show here that global mean $\Delta\delta^{13}C$ is sensitive to changes in the biogeochemical state of the Southern Ocean. We conduct four idealised sensitivity experiments with the ocean biogeochemistry general circulation model HAMOCC2s to explore the effect of biogeochemical state changes of the (Southern) Oceans on atmospheric $\delta^{13}C$, pCO_2, and marine $\delta^{13}C$ and $\Delta\delta^{13}C$. The experiments cover changes in air-sea gas exchange rates, particulate organic carbon sinking rates, sea ice cover, and nutrient uptake efficiency - in an unchanged ocean circulation field. We conclude that the maximum variation of mean marine $\Delta\delta^{13}C$ in response to (bio)geochemical change is ~0.5 ‰, which is about half of the reconstructed variation in $\Delta\delta^{13}C$ over glacial-interglacial timescales. Locally, $\Delta\delta^{13}C$ variations can surpass or even mirror the mean effects on $\Delta\delta^{13}C$ due to the spatial variation in the sensitivity of $\delta^{13}C$ to biogeochemical change. The (bio)geochemical environment of a sediment core thus needs to be well constrained in order to be able to interpret reconstructed $\Delta\delta^{13}C$ variations in such a core. The sensitivity of $\Delta\delta^{13}C$ varies spatially depending on the contribution of air-sea gas exchange versus biological export productivity to the local $\delta^{13}C$ signature. Interestingly, the direction of both glacial (intensification of $\Delta\delta^{13}C$) and interglacial (weakening of $\Delta\delta^{13}C$) $\Delta\delta^{13}C$ change matches biogeochemical processes associated with these periods. This supports the idea that biogeochemistry likely explains part of the reconstructed variations in $\Delta\delta^{13}C$, and not only ocean circulation.

1 Introduction

The vertical marine $\delta^{13}C$ gradient is the surface-to-deep difference in $\delta^{13}C$, the standardised ^{13}C isotope (Stenström et al., 2011; Stuiver and Pollack, 1977). ^{13}C is slightly heavier than the ^{12}C isotope, which causes a fractionation effect during air-sea gas exchange and biogenic carbon uptake during photosynthesis (Laws et al., 1997; Mackenzie and Lerman, 2006; Zhang et al.,

1995). This fractionation enriches dissolved inorganic carbon (DIC) at the ocean surface in $\delta^{13}C$ and it depletes the $\delta^{13}C$ in organic material (e.g. plankton). The deep sea has a depleted $\delta^{13}C$ signature in DIC as a result of remineralisation of the $\delta^{13}C$-depleted organic detritus at depth. This vertical $\delta^{13}C$ gradient is shaped by the interplay between the biological pump, air-se gas exchange and circulation (Emerson and Hedges, 2008; Zeebe and Wolf-Gladrow, 2001; Ziegler et al., 2013). The deep sea and surface ocean $\delta^{13}C$ signatures are archived in the calcareous shells of foraminifera in the sediments. Records of $\delta^{13}C$ from planktonic and benthic foraminiferal shell material cover 10s of millions of years (Hilting et al., 2008). $\delta^{13}C$ and the vertical $\delta^{13}C$ gradient ($\Delta\delta^{13}C$) have been used to reconstruct for example atmospheric carbon, ocean circulation and the strength of the biological pump (Bauska et al., 2016; Broecker and McGee, 2013; Crucifix, 2005; Curry and Oppo, 2005; Hollander and McKenzie, 1991; Hoogakker et al., 2015; Shackleton and Pisias, 1985; Zahn et al., 1986; Ziegler et al., 2013). Note that $\Delta\delta^{13}C$ is independent of whole-ocean $\delta^{13}C$ shifts (due to terrestrial influences) because such influences would affect $\delta^{13}C$ equally everywhere. Contemporary measurements of $\delta^{13}C$ of dissolved inorganic carbon (DIC) support the quantification of anthropogenic carbon uptake by the oceans as well as the study of the effects of biology and ocean circulation on tracer distributions (Eide et al., 2017b; Gruber and Keeling, 2001; Holden et al., 2013; Kroopnick, 1980; Kroopnick, 1985; Quay et al., 2003). However, major uncertainties remain in the interpretation of foraminiferal $\delta^{13}C$ records and $\Delta\delta^{13}C$ (Broecker and McGee, 2013; Oliver et al., 2010) as well as in the interpretation of the present day $\delta^{13}C$ data (Eide et al., 2017b).

This article addresses part of these uncertainties by exploring the pre-industrial sensitivity of $\delta^{13}C$ and $\Delta\delta^{13}C$ to (bio)geochemical change in idealised model experiments. By doing so we can investigate a number of (bio)geochemical mechanisms that could explain (part of) the observed changes in $\delta^{13}C$ and $\Delta\delta^{13}C$. We focus on the Southern Ocean (SO), the ocean south of 45° S, because the SO plays an important role in the global carbon cycle by regulating atmospheric CO_2 concentrations and uptake of anthropogenic CO_2 (Broecker and Maier-Reimer, 1992; Heinze, 2002; Marinov et al., 2006) as well as influencing the global efficiency of the biological pump, global primary production and preformed nutrients (Primeau et al., 2013).

Variations in $\Delta\delta^{13}C$ over the past few 100 000 years show that $\Delta\delta^{13}C$ is increased during glacials and reduced during interglacials (Charles et al., 2010; Oliver et al., 2010). These variations have been explained by ocean circulation changes associated with sea ice formation due to lower glacial temperatures around Antarctica and consecutive stratification (Jansen, 2017). However, not all tracers support a change in circulation (Charles et al., 2010) and processes other than ocean circulation/stratification are likely needed to explain $\Delta\delta^{13}C$ variability (Ziegler et al., 2013).

Here, we explore the sensitivity of $\delta^{13}C$ and $\Delta\delta^{13}C$ to changes in the (bio)geochemical state of the Global Ocean and Southern Ocean. Our results aim to support the paleo-oceanographic interpretation of $\delta^{13}C$ and $\Delta\delta^{13}C$ as well as the understanding of the dominant SO role in global carbon cycling and its variability and sensitivity. In order to study different (bio)geochemical mechanisms that could influence $\delta^{13}C$ and $\Delta\delta^{13}C$, a set of sensitivity experiments is designed in the ocean biogeochemistry general circulation model HAMOCC2s (Heinze et al., 2016). The experiments each focus on one or more of the (bio)geochemical aspects described to be important for $\delta^{13}C$ and $\Delta\delta^{13}C$, e.g. the biological pump efficiency and/or equilibration at the air-sea interface (Sect. 3.3.1-3.3.4). Together these experiments provide a broad spectrum of (bio)geochemical changes

Biogeosciences Discuss., https://doi.org/10.5194/bg-2018-52
Manuscript under review for journal Biogeosciences
Discussion started: 26 February 2018

that could influence local and global $\delta^{13}C$ and $\Delta\delta^{13}C$. An approximation is made of the contribution of biology versus air-sea gas exchange to $\delta^{13}C$ (Sect. 3.2). The modelling results of Sect. 3.3.1-3.3.4 are discussed and compared with observational data from sediment cores (Sect. 3.4). As $\delta^{13}C$ and $\Delta\delta^{13}C$ are used to study changes in atmospheric pCO_2 (pCO_2^{atm}), a final section will cover the changing relationship between $\delta^{13}C$, $\Delta\delta^{13}C$ and pCO_2^{atm} under different marine (bio)geochemical states (Sect. 3.5).

2 Methods

In this study we employ the ocean biogeochemistry general circulation model HAMOCC2s (Heinze et al., 2016) which simulates the inorganic and organic carbon cycle in the water column and in the sediments. The horizontal resolution of the model is 3.5° × 3.5° and there are 11 depth layers in the ocean. HAMOCC2s has an annual time step and an annually averaged fixed circulation field, as well as a free box atmosphere for O_2, $^{13}CO_2$ and CO_2. The model is computationally very economic and thus an ideal tool for sensitivity experiments over long integration times. Biological particles in the model are particulate organic carbon (POC), calcium carbonate and biogenic silica. POC and opal production are described using Michaelis-Menten kinetics for nutrient uptake, limited by phosphate and silicic acid (Heinze et al., 1999). POC is carried as a tracer as well as transported downwards according to an exponential particle penetration profile and a constant sinking velocity, thereby consuming oxygen (i.e. remineralisation of POC with depth). As the model has an annual time step, sea ice is always present south of ~60° S and north of ~70° N in the control run (Fig. S1). More details about the model are provided in previous studies using a similar configuration of HAMOCC2 (Heinze, 2002; Heinze et al., 2016).

Fractionation during photosynthesis is set to a constant -20 ‰ (Lynch-Stieglitz et al., 1995; Tagliabue and Bopp, 2008) as model results are little influenced by the chosen parameterisation (Jahn et al., 2015; Schmittner et al., 2013). The fractionation during air-sea gas exchange depends on temperature according to ε=-9.483/T + 23.89 ‰ (Mook, 1986), causing stronger fractionation at lower temperatures (i.e. at high latitudes). Fractionation during $CaCO_3$ formation is omitted from the model as done in previous studies (Lynch-Stieglitz et al., 1995; Marchal et al., 1998; Schmittner et al., 2013) as its size is uncertain but likely minor (~1 ‰) and effects on $\delta^{13}C$ and $\Delta\delta^{13}C$ are small (Shackleton and Pisias, 1985). In the version of HAMOCC2 used in this study, a fixed weathering input is used to tune the ocean inventory to values comparable to observations. The 'best-fit' weathering value was found by running the model with a restored (to a value of -6.5 ‰) atmospheric $\delta^{13}C$ until the prognostic burial rate reached equilibrium with weathering (after ~110000 model years). Consecutively, the atmospheric restoring was removed to create a free atmosphere model setup with close-to-observed marine and atmospheric $\delta^{13}C$ values. This equilibrated model version is referred to as the 'control run' in the remainder of this article. We define the vertical $\delta^{13}C$ gradient ($\Delta\delta^{13}C$) as:

$$\Delta\delta^{13}C = \delta^{13}C_{surface} - \delta^{13}C_{deep}\ , \quad (1)$$

Biogeosciences Discuss., https://doi.org/10.5194/bg-2018-52
Manuscript under review for journal Biogeosciences
Discussion started: 26 February 2018

where $\delta^{13}C_{surface}$ and $\delta^{13}C_{deep}$ are the volume-weighted mean $\delta^{13}C$ in the surface ocean (<250m depth) and the deep ocean (>250m depth), respectively. By doing so, we can compare the $\Delta\delta^{13}C$ summarised as one number between the different sensitivity experiments.

We conducted four sensitivity experiments to explore changes in air-sea gas exchange rate, sea ice extent (influencing both biological production and the air-sea gas exchange of carbon) and the efficiency of the biological pump through the POC sinking rate and nutrient uptake rate (Table 1). This article employs the term 'efficiency of the biological pump' as a measure of the success of phytoplankton to maintain low nutrient concentrations in the surface ocean. All experiments are run for 2000 model years starting from the end of the spinup. The gas exchange rate and POC sinking rate experiments are done twice, once changing the respective model parameter for the Global Ocean and once only for the Southern Ocean (SO-only). The model parameters where changed in a way that marine biogeochemical tracer distributions (e.g. PO_4^{3-}, $\delta^{13}C$) remained reasonable but did provide an estimate of the sensitivity of the respective tracer to (bio)geochemical change. The maximum and minimum sea ice cover experiments approximate the Last Glacial Maximum winter extent and the modern summer extent of SO sea ice, respectively (Crosta (2009) and Fig. A22 therein).

The contribution of biological processes versus air-sea gas exchange to $\delta^{13}C$ is calculated using the method of Broecker and Maier-Reimer (1992) as done for observations by Eide et al. (2017b) and in a modelling context by Sonnerup and Quay (2012):

$$\delta^{13}C_{bio}[‰] = \frac{\varepsilon_{photo}}{\overline{DIC}} * r_{c:p} * (PO_4 - \overline{PO_4}) + \overline{\delta^{13}C}\ , \quad (2)$$

where $\varepsilon_{photo} = -20$ ‰, $r_{c:p} = 122$ and the following model control run mean values are used: $\overline{DIC} = 2308.793\ \mu mol/kg$, $\overline{PO_4} = 2.399\ \mu mol/kg$ and $\overline{\delta^{13}C} = 0.742$ ‰. These values result in the modelled $\delta^{13}C_{bio}$:PO_4^{3-} relationship $\delta^{13}C_{bio}$=3.4-1.1* PO_4^{3-}. The constant 3.4 is somewhat higher than estimated for observed $\delta^{13}C$ for which a constant of 2.8 was found by Eide et al. (2017b). This higher constant originates from the over-prediction of the model of mean $\delta^{13}C$ and PO_4^{3-} at depth, as seen in other models (Sonnerup and Quay, 2012). Eq. (2) assumes a constant biological fractionation as well as a constant $r_{c:p}$ ratio, and these assumptions will introduce some error in the partition of biological and air-sea gas exchange signatures derived from observed $\delta^{13}C$ to PO_4^{3-} ratios (e.g., Eide et al. 2017). For the purpose of determining $\delta^{13}C_{bio}$ in our model, these assumptions are unproblematic, since $r_{c:p}$ and ε_{photo} actually are taken to be constant in the model formulation. The air-sea gas signature $\delta^{13}C_{AS}$ is approximated as the residual ($\delta^{13}C_{AS} = \delta^{13}C_{model} - \delta^{13}C_{bio}$). $\delta^{13}C_{AS}$ is 0 ‰ when $\delta^{13}C_{model}=\delta^{13}C_{bio}$, i.e. when the $\delta^{13}C$ can be explained by biology only. To aid interpretation of the results, we express $\delta^{13}C_{bio}$ as a percentage as $\delta^{13}C_{bio}^{perc}$ because the absolute values in ‰ depend strongly on the chosen 'reference' values, i.e. mean DIC, PO_4^{3-}, and $\delta^{13}C$ (compare Schmittner et al., 2013; Sonnerup and Quay, 2012; Broecker and Maier-Reimer, 1992; Lynch-Stieglitz et al., 1995; Eide et al., 2017b). The conversion from $\delta^{13}C_{bio}$ to a percentage is calculated as follows:

$$\delta^{13}C_{bio}^{perc}[\%] = \frac{|\delta^{13}C_{bio}|}{|\delta^{13}C_{bio}|+|\delta^{13}C_{AS}|} * 100\ \% \quad (3)$$

Biogeosciences Discuss., https://doi.org/10.5194/bg-2018-52
Manuscript under review for journal Biogeosciences
Discussion started: 26 February 2018

In our analysis, we define the total amount of air-sea carbon exchange as $F_{u+d}=|F_{up}|+|F_{down}|$, with F_{up} as the upward annual carbon flux from the ocean into the atmosphere and F_{down} its downward counterpart. F_{u+d} is relevant for understanding the sensitivity of $\delta^{13}C$. The net carbon exchange is defined as $F_{net}=F_{up}+F_{down}$. The sign of F_{net} indicates whether a region is a source or a sink for carbon and is relevant for understanding changes in atmospheric pCO_2^{atm}.

3 Results and discussion

3.1 Model control run

The model reproduces the main features of observed marine $\delta^{13}C$, as shown in Fig. 1 and Fig. S2. The modelled surface ocean $\delta^{13}C$ is enriched (1.6 ‰ average above 250 m depth) and the deep ocean $\delta^{13}C$ is more depleted (0.7 ‰ average below 250 m depth). The mean ocean $\Delta\delta^{13}C$ is thus 0.9 ‰. The mean modelled ocean $\delta^{13}C$ is over-predicted by 0.2 ‰ relative to observations (Eide et al., 2017b), which is especially pronounced in the oldest water masses (Fig. S2). This is observed in other models as well and attributed to the model's relative contribution of deep water production in the North Atlantic and Southern Ocean (Sonnerup and Quay, 2012). The modelled global POC production is 9.6 Gt C yr^{-1} of which 18 % is produced in the SO, which is within the uncertainty of observational estimates (MacCready and Quay, 2001; Nevison et al., 2012; Dunne et al., 2007; Lutz et al., 2007; Schlitzer, 2002). The free atmosphere has a modelled equilibrium pCO_2^{atm} of 279 ppm and a $\delta^{13}C$ of -6.44 ‰ which developed in the model from the 'best-fit' weathering value as described above in Sect. 2. Net air-sea gas exchange is close to zero (ventilating ~5×10^{-6} Pg of carbon to the atmosphere annually), indicating that the model is in equilibrium. The resulting drift of the model control over 2000 years is $+7\times10^{-3}$ ‰ for both $\delta^{13}C^{atm}$ and mean marine $\delta^{13}C$, and $+5\times10^{-3}$ ppm for pCO_2^{atm}.

3.2 Air-sea gas exchange versus biology

The contribution of biology based on equations (2) and (3) to the $\delta^{13}C$ distribution is presented in Fig. 2. Our results agree with previous studies on the relative role of biology and ocean circulation to the $\delta^{13}C$ distribution (Kroopnick, 1985; Schmittner et al., 2013). The contribution of biology to the modelled $\delta^{13}C$ distribution is generally below 45 % and has a steep gradient from the surface to the deep ocean. The (thermodynamic) fractionation effect of air-sea gas exchange on $\delta^{13}C$ is strongly impeded by the long equilibration time of ^{13}C, which results in room for biological processes to contribute significantly to $\delta^{13}C$ and $\Delta\delta^{13}C$ (Eide et al., 2017a; Lynch-Stieglitz et al., 1995; Schmittner et al., 2013). In the deep ocean below 250m, the influence of biology increases to 35-45 % due to the remineralisation of POC, with the exception of the Arctic Ocean where no POC production is modelled due to the sea ice cover (Fig. 2b and Fig. S1). $\delta^{13}C_{bio}^{perc}$ is close to 50 % around 1000m depth in the northern Pacific and Indian oceans, due to the old water masses located there, which have accumulated a large fraction of remineralised DIC. At the surface, air-sea gas exchange dominates the $\delta^{13}C$ signature of DIC as visible from the low $\delta^{13}C_{bio}^{perc}$ (Fig. 2a). The only exception at the surface is in upwelling regions, where a relatively high $\delta^{13}C_{bio}^{perc}$ is expected due to high

POC production and upwelled remineralised carbon. High $\delta^{13}C_{bio}^{perc}$ generally corresponds to a $\delta^{13}C$ depleted water mass (compare Fig. 1 and Fig. 2), as expected from the upwelling of $\delta^{13}C$ depleted DIC and modelled and observed close to the Antarctic continent (Fig. 1a and observations by Eide et al. (2017a)). The results presented in Fig. 2 appear to be quite robust as $\delta^{13}C_{bio}^{perc}$ typically does not change more than 5-10 % for the wide range of biogeochemical states as explored in the sensitivity experiments presented below.

3.3 Sensitivity of Δδ13C and $\delta^{13}C$

3.3.1 Air-sea gas exchange of carbon

Atmospheric and marine $\delta^{13}C$ are generally in thermodynamic disequilibrium because ^{13}C equilibrates ~200 times slower than inert gases like O_2. This difference in equilibration time is due to the fact that ^{12}C needs to speciate into all marine carbon species to reach equilibrium (~20x slower than O_2), after which ^{13}C needs to go through full isotopic exchange between all carbon species to reach equilibrium (~10x slower than ^{12}C) (Jones et al., 2014; Galbraith et al., 2015). The extent of this $\delta^{13}C$ disequilibrium archives the ventilation time of that water parcel, thereby making $\delta^{13}C$ a good tracer for water mass circulation (Eide et al., 2017b). The surface ocean $\delta^{13}C$ signature is dominated by air-sea gas exchange in most ocean regions (Fig. 2). Any change in the gas exchange rate can thus potentially have a large effect on surface ocean $\delta^{13}C$, depending on the prior disequilibrium.

The gas exchange experiments (Sect. 2, Table 1) result in profound changes in the $\delta^{13}C$ distribution, the $\Delta\delta^{13}C$ as well as $\delta^{13}C^{atm}$ and pCO_2^{atm}. pCO_2^{atm} is governed by the transient change in the net air-sea gas exchange flux F_{net}, which occurs until a new equilibrium is established. We find an increase of pCO_2^{atm} by 9 ppm (fast gas exchange) and by 4 ppm (slow gas exchange), respectively. If gas exchange is only changed in the SO (i.e. for 22% of the global ocean area), an effect of 5 ppm and 1 ppm increase is found (Table 2). The spatially variable prior pCO_2 disequilibrium in the SO plays an important role in the atmospheric pCO_2 sensitivity: The larger increase of the outgassing flux F_u of the SO as compared to the carbon uptake flux F_d leads to a reduced SO carbon sink and higher pCO_2^{atm} at increased gas exchange rates. Interestingly, the $\delta^{13}C^{atm}$ gets decoupled from the pCO_2^{atm} signal as $\delta^{13}C^{atm}$ decreases (to -6.8 ‰) during fast gas exchange and increases (to -6.3 ‰) when the gas exchange rate is reduced. This is explained by the increase in the global amount of air-sea gas exchange F_{u+d} in the fast gas exchange experiment. Such an increase leads to a smaller thermodynamic disequilibrium, which enriches the mean marine $\delta^{13}C$ and depletes $\delta^{13}C^{atm}$. The opposite occurs for the slow gas exchange experiment. Moreover, our SO-only experiments show that these effects on the atmosphere are more pronounced if gas exchange only changes in the SO. This indicates that the remainder of the ocean offsets part of the atmospheric sensitivity to SO change.

In the ocean, $\delta^{13}C$ shows a different response in high latitudes as compared to the lower latitudes in the surface ocean (Fig. 3a): An increased air-sea gas exchange rate lowers the surface ocean $\delta^{13}C$ -0.2 to -0.9 ‰ in the lower latitudes and increases surface ocean $\delta^{13}C$ in high latitudes by 0.2-0.5 ‰. These results indicate the sign of the thermodynamic $\delta^{13}C$ disequilibrium between surface ocean and atmosphere. In line with previous studies (Schmittner et al., 2013; Galbraith et al., 2015) the

disequilibrium is negative ($\delta^{13}C < \delta^{13}C_{eq}$) at high latitudes and in low latitude upwelling regions, and positive elsewhere. The net effect of a slower gas exchange rate on surface ocean $\delta^{13}C$ is less pronounced and reversed to the effects discussed for an increased gas exchange rate (not shown). The smaller effects seen for slow gas exchange indicate that the control model ocean is a 'slow ocean', i.e. closer to (very) slow gas exchange than to thermodynamic equilibrium (fast gas exchange).

The effect of the gas exchange rate on marine $\delta^{13}C$ is mostly established in the top 250-1000 m of the water column (Fig. 3c, d). The sensitivity of $\Delta\delta^{13}C$ to the gas exchange rate therefore mainly depends on surface ocean $\delta^{13}C$. On average, the $\Delta\delta^{13}C$ weakens to 0.65 when the thermodynamic disequilibrium is decreased (i.e. 'Gas fast', Fig. 4) and $\Delta\delta^{13}C$ strengthens to 1.00 when the thermodynamic disequilibrium is increased ('Gas slow', Fig. 4). The extent to which thermodynamic equilibrium can develop is thus an efficient way to change the biologically induced $\Delta\delta^{13}C$. Note that local changes in the $\Delta\delta^{13}C$ can be different from the global mean vertical gradient, and can be more pronounced (subtropical gyres in Fig. 3a). Importantly, in the SO the $\Delta\delta^{13}C$ signal has an opposite sign of the global mean: The $\Delta\delta^{13}C$ is strengthened south of about 40°S when the thermodynamic disequilibrium is decreased (Fig. 3a). Note as well that the SO surface ocean enrichment is compensated in low latitude regions (compare Fig. 3a, b).

3.3.2 The biological pump: POC sinking rate

The net effect of a regionally changed biological pump efficiency depends on the sequestration efficiency, which depends on the interplay between the biological pump and ocean circulation (DeVries et al., 2012). A more efficient biological pump (here, a higher POC sinking rate) leads to a loss of carbon to the sediments, which dominates the effects on pCO_2^{atm} and $\delta^{13}C^{atm}$. The sediment burial causes efficient long-term removal of carbon from the active carbon cycle which leads to a 28 ppm reduction of pCO_2^{atm} and relatively higher (-6.2 ‰) atmospheric $\delta^{13}C$ (Table 2) as well as a shift of the mean ocean $\delta^{13}C$ by ~0.15 ‰. Besides that, an efficient biological pump leads to a global ~10 % decrease in the amount of air-sea gas exchange F_{u+d} because of reduced POC production as surface waters are depleted of nutrients. A mirrored but weaker response is modelled for a decrease in biological pump efficiency. Halving the POC sinking rate leads to a 13 ppm increase in pCO_2^{atm} (of which 28 % can be explained by the SO) and a more negative atmospheric $\delta^{13}C$ (-6.7 ‰) and increased F_{u+d} (Table 2).

Surface ocean $\delta^{13}C$ is mostly influenced by the changes in productivity and the vertical displacement of the remineralisation horizon. POC sinking removes nutrients and light ^{12}C carbon from the surface ocean, while exporting them to the deep ocean. This leaves the surface ocean more enriched in $\delta^{13}C$ and the deep ocean more depleted if POC sinking rates are high, despite the overall increase in marine $\delta^{13}C$ (Fig. 5a). Therefore, even though the absolute export production is reduced in all productive regions (-26 %), the biological pump is more efficient as any new nutrients in the surface ocean will immediately be used and exported. When reducing the biological pump efficiency both remineralisation and POC production are confined to the surface ocean. The net effect is that the surface ocean becomes more depleted in $\delta^{13}C$, as the fractionation effect during photosynthesis is counteracted by the remineralisation of POC (which would normally have occurred at depth). The SO plays a relatively minor role in these changes (Fig. 5b). This suggests that the POC export production of the SO is less determined by the local POC sinking rate than elsewhere. Changes in deep ocean $\delta^{13}C$ depend on the water mass age (Fig. 5c). Old water (North

Pacific) has a larger remineralisation signal when the biological pump is efficient. Independent of the biological pump efficiency, the relatively young waters of the deep North Atlantic seem to generally adopt about the same $\delta^{13}C$ signal as the surface ocean $\delta^{13}C$, which is set by air-sea gas exchange. This is in agreement with a relatively low $\delta^{13}C_{bio}^{perc}$ estimate for the deep North Atlantic (~30 %).

From Fig. 5 we observe that the sensitivity of the $\Delta\delta^{13}C$ strongly depends on location. In general, the $\Delta\delta^{13}C$ strengthens for an increased biological pump efficiency, and this effect is stronger with water mass age (Fig. 5c). The opposite happens for a reduced biological pump efficiency, which weakens the $\Delta\delta^{13}C$ (Fig. 5). It is worth noting, however, that the changes in $\Delta\delta^{13}C$ in the SO are comparably small. In the North Pacific, where the changes in the $\Delta\delta^{13}C$ are most pronounced, this is mostly due to the surface ocean sensitivity because the deep ocean changes are small compared to the surface ocean changes.

3.3.3 The biological pump: SO nutrient depletion

Consistent with previous studies (Primeau et al., 2013; Marinov et al., 2006; Sarmiento et al., 2004), we find a large atmospheric impact in our SO nutrient depletion experiment. The high SO nutrient uptake efficiency (i.e. an efficient biological pump) maintains a 28 ppm reduction in pCO_2 as seen similarly for the efficient biological pump experiment with a high POC sinking rate (Sect. 3.3.2). However, $\delta^{13}C^{atm}$ behaves differently in the V_{max} experiment than in the efficient biological pump experiment based on POC sinking rates: An increased POC sinking rate leads to a $\delta^{13}C^{atm}$ increase of ~0.2 ‰ due to export of light organic carbon to the sediments (Sect. 3.3.2). In contrast, in the V_{max} experiment $\delta^{13}C^{atm}$ reduces by ~0.2 ‰ to -6.6 ‰. In the SO, carbon outgassing to the atmosphere (F_{up}) is reduced by nearly 40 % because the high nutrient and carbon consumption do not permit CO_2 to escape to the atmosphere. This plays a key role in the globally 10 % reduced air-sea exchange, both because of its magnitude and because of stronger thermodynamic fractionation in high latitudes.

The global export production of POC becomes confined to the SO due to the high nutrient uptake rate and the local 5-fold increase in POC production. This causes a range of effects on the distribution of $\delta^{13}C$. First, the high POC export in the SO leaves the SO surface ocean enriched in $\delta^{13}C$ and depletes the deep ocean due to remineralisation. This deep SO remineralisation signal is then carried northward with Antarctic Bottom Water into all ocean basins (Fig. 6b, c) and under the sea ice at the surface of the SO (Fig. 6a). Furthermore, the efficient export of carbon to the deep ocean causes the SO to become a much stronger sink for atmospheric carbon (~11x stronger, Fig. S3). Parts of this excess carbon is ventilated back to the atmosphere at lower latitudes (Fig. S3). Productivity and thus POC export and remineralisation are strongly reduced outside of the SO (~10 % global decrease in POC export production). The reduced productivity and export is consistent with previous studies (Primeau et al., 2013; Marinov et al., 2006; Sarmiento et al., 2004), which causes surface ocean $\delta^{13}C$ to become relatively depleted and deep ocean $\delta^{13}C$ to become relatively enriched as compared to the control (Fig. 6b, c). This relatively enriched deep ocean signal surfaces in upwelling regions around the equator and in the Arctic (Fig. 6a). As for the $\delta^{13}C^{atm}$, the mean marine $\delta^{13}C$ is reduced in the V_{max} experiment because the SO, Pacific and Indian deep oceans are filled with a stronger remineralisation signature (Fig. 6b, c). $\Delta\delta^{13}C$ is thus strongly increased in the SO between 60 and 40°S, but decreased or

unchanged in the North Atlantic. In the Pacific, there is a pattern with an increase in intermediate water masses, and a decrease at the surface and at depth.

3.3.4 Southern Ocean sea ice cover

The sea ice cover of the SO changes considerably over glacial-interglacial cycles, as well as on seasonal timescales (Crosta (2009) and Fig. A22 therein). In general, a sea ice cover will inhibit light penetration into the surface ocean as well as air-sea gas exchange. Here we assume complete inhibition of both light and air-sea carbon exchange by sea ice. In this section we thus explore the effect of both biological production and air-sea gas exchange in two extreme cases, i) the largest realistic sea ice cover based on the glacial maximum winter extreme (50° S) and ii) the smallest sea ice cover based on the contemporary summer minimum sea ice extent (70° S). Note that there is a constant sea ice cover about north of 70°N and south of 60° S in the control run of the model. Therefore, the strongest marine $\delta^{13}C$ change is expected south of 60° S for a decreased sea ice cover and between 50-60° S for an increased sea ice cover, as this is the area where ice cover is altered relative to the control run.

Both local and global air-sea carbon fluxes are influenced by a change of the SO sea ice cover, which results in changes in pCO_2^{atm} and $\delta^{13}C$. In our experiment, pCO_2^{atm} increases by 5 ppm for an increased sea ice cover and decreases by 5 ppm for a decreased sea ice cover (Table 2). As noted in Sect. 3.3.1, a change in pCO_2^{atm} is governed by a transient change in the net air-sea gas exchange flux F_{net} until a new equilibrium is established. Initially, an extended ice cover causes more CO_2 to remain in the atmosphere because the additional ice covers a part of the SO that is a sink for CO_2 (Fig. S4). As the net global air-sea gas exchange F_{net} approaches equilibrium, the non-SO ocean therefore becomes a smaller source for carbon. This reduces the net gas exchange F_{net} inside and outside of the SO by about one third. Our results show that the effects of an extended sea ice cover on pCO_2^{atm} strongly depends on the location of the sea ice edge: Stephens and Keeling (2000) for example modelled a strong decrease of pCO_2^{atm} in response to an increased sea ice cover south of the Antarctic Polar Front.

The reduction in pCO_2^{atm} by 5 ppm due to a reduced sea ice cover is fully attributable to the POC production in the earlier ice-covered area between ~60° S and 70° S. If the ice would just influence air-sea gas exchange, the sea ice retreat would lead to an increase in pCO_2^{atm} because the region below the ice is strongly supersaturated in C with respect to the atmosphere (Fig. S4). The increased sea ice cover leads to a complete suppression of air-sea gas exchange south of 50°S. Since this region is in negative disequilibrium with the atmosphere ($\delta^{13}C < \delta^{13}C_{eq}$, compare Fig. 2), the ice cover inhibits a $\delta^{13}C$ flux into the ocean. As a result, $\delta^{13}C^{atm}$ increases to -6.14 ‰, and the opposite happens for a reduced sea ice cover, leading to a lowered $\delta^{13}C^{atm}$ (-6.57 ‰).

The increased sea ice cover over the SO results in a surface ocean $\delta^{13}C$ depletion relative to the control of -0.5 ‰ to -0.1 ‰ in the SO, while $\delta^{13}C$ is enriched outside of the SO with 0-0.2 ‰ (Fig. 7a). The depletion is especially pronounced between 40-60° S. The ~40 % reduced POC export production in the SO due to light inhibition by the sea ice cover causes a major part of the SO surface $\delta^{13}C$ depletion, as the absence of photosynthesis will leave the surface ocean less enriched in $\delta^{13}C$. Next to less enrichment from biological production, the reduced air-sea gas exchange F_{u+d} in the SO also leads to a more depleted surface

ocean $\delta^{13}C$ signature. About the opposite happens when we simulate a strongly decreased sea ice cover (only ice south of 70° S): A small depletion of $\delta^{13}C$ is modelled outside the SO, but the SO $\delta^{13}C$ locally becomes up to ~0.8 ‰ enriched relative to the control (Fig. 7b) as the increased amount of air-sea gas exchange F_{u+d} in the newly exposed area leaves the surface ocean enriched in $\delta^{13}C$ during fractionation.

The effect of a changed ice cover on deep ocean $\delta^{13}C$ is less than ~0.1 ‰ (Fig. 7a, b) as the surface signal is diluted while it follows the general ocean circulation. Global mean $\Delta\delta^{13}C$ is therefore not significantly affected by changes in the SO sea ice cover (Fig. 4). Locally in the SO, however, the $\Delta\delta^{13}C$ weakens considerably when the 50-60° S region becomes covered with sea ice and strengthens considerably between 60-70° S if the sea ice is removed.

3.4 Modelled versus observed $\Delta\delta^{13}C$ variations

The variations in $\Delta\delta^{13}C$ on glacial-interglacial timescales provide researchers with a tracer to study the biogeochemical state of the past global ocean, under the condition that we can interpret (variations in) $\Delta\delta^{13}C$. This study shows that the sensitivity of $\Delta\delta^{13}C$ depends on location, which is in agreement with the often incoherent patterns of ocean basin planktonic and benthic foraminiferal $\delta^{13}C$ (Oliver et al., 2010). The idealised and large perturbations made to the biogeochemical state of the (Southern) Ocean in this study show that mean $\Delta\delta^{13}C$ varies no more than ~0.5 ‰ (Fig. 4) under the assumption of a constant ocean circulation. Locally however, larger variations in $\Delta\delta^{13}C$ can occur. $\Delta\delta^{13}C$ reconstructions based on sediment core $\delta^{13}C$ data show $\Delta\delta^{13}C$ variations of ~1 ‰ over the past 350 000 years (Shackleton and Pisias, 1985; Ziegler et al., 2013; Charles et al., 2010; Oliver et al., 2010). Ocean circulation changes explain at least part of these variations in $\Delta\delta^{13}C$ (Charles et al., 2010; Heinze et al., 1991; Jansen, 2017; Heinze and Hasselmann, 1993). However, the changes in the biogeochemical state of the ocean imposed in our experiments show that reconstructed variations in $\Delta\delta^{13}C$ may be strongly influenced by (bio)geochemical change. Rapid changes of a large magnitude are expected in the SO carbon cycle from the pCO_2 and $\Delta\delta^{13}C$ records (Ziegler et al., 2013). We propose that this reconstructed intra-millennial variability in $\Delta\delta^{13}C$ could be driven more by changes in the biogeochemical state than by changes in ocean circulation because (bio)geochemical changes might occur more rapidly than whole-ocean circulation changes. Analysis of SO $\Delta\delta^{13}C$ reconstructions from sediment cores at 42° S and 46° S (Charles et al., 2010) shows that there is a strong correlation between these cores and Northern Hemisphere $\Delta\delta^{13}C$ variations. Based on the local character of the $\Delta\delta^{13}C$ sensitivity, we expect that this strong correlation does not exist for cores further south in the SO: The SO south of ~50-60° S often has a different $\Delta\delta^{13}C$ response to (bio)geochemical change than the rest of the oceans (this study). This difference may be attributed to the existence of the biogeochemical divide (Marinov et al., 2006).

In general, the reconstructed $\Delta\delta^{13}C$ is increased during glacials and reduced during interglacials (Charles et al., 2010; Oliver et al., 2010; Ziegler et al., 2013). This variation is best supported by data for the North Atlantic, as data are too sparse in other basins to get a coherent picture of $\Delta\delta^{13}C$ variations (Oliver et al., 2010). The results of this study show that fast gas exchange or an inefficient biological pump are candidates to contribute to the reduction of mean $\Delta\delta^{13}C$ (Fig. 4), but the reduction is found for low latitudes only. In the SO, $\Delta\delta^{13}C$ is not very sensitive (POC sinking) or even reversed (fast gas exchange). Interglacial periods, when $\Delta\delta^{13}C$ is reduced, are generally thought to be associated with a decrease in the efficiency of the

biological pump and increased deep-ocean ventilation via southern-sourced water masses (Gottschalk et al., 2016). Increased deep-ocean ventilation might be driven by increased winds, which we can associate with increased gas exchange rates. Each of these processes indeed reduces $\Delta\delta^{13}C$ in the mean (Fig. 4). However, the interglacial reduction of $\Delta\delta^{13}C$ seems to originate from deep sea $\delta^{13}C$ enrichment (Charles et al., 2010; Oliver et al., 2010). Our results show that neither an inefficient biological pump nor fast gas exchange can be associated with a pronounced deep sea $\delta^{13}C$ increase as their effects are restricted to the surface ocean. Besides that, $\Delta\delta^{13}C$ is only increased in lower latitudes for fast gas exchange rates and the effects of a reduced efficiency of the biological pump on $\Delta\delta^{13}C$ is both vertically and horizontally variable.

Regarding glacials, our results show that an increase in mean $\Delta\delta^{13}C$ could (bio)geochemically come from slow gas exchange, high POC sinking rates, or efficient nutrient consumption in the SO (Fig. 4). Such biogeochemical changes have been associated with glacial periods (for example, Ziegler et al. (2013)) and are, therefore, potential candidates to explain part of the $\Delta\delta^{13}C$ increase in interplay with stronger ocean stratification. Sediment-core reconstructions of $\Delta\delta^{13}C$ show that an increased $\Delta\delta^{13}C$ can originate either from a mid-depth (1200 m, at 42° S and 46° S) increase in $\delta^{13}C$ (Charles et al., 2010) or a general deep ocean $\delta^{13}C$ decrease (Oliver et al., 2010). A deep sea $\delta^{13}C$ decrease is associated with North-Pacific waters of an efficient biological pump (V_{max} and high POC sinking rate experiments). The effects on $\delta^{13}C$ of slow gas exchange are limited to the surface ocean and $\Delta\delta^{13}C$ is only increased in lower latitudes.

3.5 The changing relationship between $\Delta\delta^{13}C$, $\delta^{13}C^{atm}$ and pCO_2^{atm}

One would expect variations of surface water $\delta^{13}C$ as well as $\Delta\delta^{13}C$ to correlate with variations in pCO_2^{atm}, because similar processes (biology and air-sea gas exchange) steer their distribution/concentrations (Shackleton and Pisias, 1985; this article). Here we show that a rough relationship between $\delta^{13}C^{atm}$ and $\Delta\delta^{13}C$ holds over a wide range of (bio)geochemical states, as simulated in the sensitivity experiments. Figure 8a shows that changes in the POC sinking rate lie approximately along a line in $\delta^{13}C^{atm}$:$\Delta\delta^{13}C$ space. In contrast to that, changes in air-sea gas exchange (as simulated in the gas exchange and sea ice cover experiments) affect $\delta^{13}C^{atm}$ more than $\Delta\delta^{13}C$. This confirms the idea that $\Delta\delta^{13}C$ is governed by biological processes and will also set $\delta^{13}C^{atm}$, unless air-sea gas exchange gets the chance to dominate $\delta^{13}C^{atm}$. The air-sea gas exchange effect depends on the interplay between thermodynamic disequilibrium and gas exchange rates, see Sect. 3.3.1 and Fig. 3. A statistically significant relationship was also found across the sensitivity experiments between pCO_2^{atm} and global mean $\Delta\delta^{13}C$ (Fig. 8b). A local correlation between $\Delta\delta^{13}C$ and pCO_2^{atm} (such as found by for example Dickson et al. (2008)) can thus both be attributed to changes in the (bio)geochemical state and ocean stratification.

4 Summary and conclusions

This study addressed the governing processes and sensitivity of $\delta^{13}C$ and $\Delta\delta^{13}C$, focusing on the contribution of the SO. Using the ocean biogeochemistry general circulation model HAMOCC2s, a set of four sensitivity experiments gave insight in the effects of (bio)geochemical change on $\delta^{13}C$ and $\Delta\delta^{13}C$. The results show the important role of the SO in global $\delta^{13}C$ and the

$\Delta\delta^{13}C$ sensitivities as well as the strong spatial differences in sensitivity. The $\delta^{13}C$ signature is governed by different processes depending on location. Air-sea gas exchange sets surface ocean $\delta^{13}C$ in all ocean basins, contributing 60-100 % to the $\delta^{13}C$ signature. At depth and with increasing water mass age, the influence of biology increases to 50 % due to POC remineralisation. This spatial diversity of the processes behind the $\delta^{13}C$ signature of a water parcel results in a non-uniform sensitivity of $\delta^{13}C$ to (bio)geochemical change.

Both $\delta^{13}C^{atm}$ and surface ocean $\delta^{13}C$ are strongly influenced by changes in the amount of air-sea gas exchange F_{u+d}, since this sets the $\delta^{13}C$ atmosphere ocean disequilibrium, whereas pCO_2^{atm} is influenced by net outgassing or uptake of carbon F_{net}. There generally is a stronger thermodynamic disequilibrium between the surface ocean and the atmosphere for $\delta^{13}C$ than for pCO_2. Regional differences in the thermodynamic disequilibrium of $\delta^{13}C$ and pCO_2 are therefore found to cause decoupling of the $\delta^{13}C^{atm}$ and pCO_2^{atm} sensitivity response. A significant relationship was however found across the sensitivity experiments between pCO_2^{atm} and $\Delta\delta^{13}C$. This result shows that paleo-reconstructions of pCO_2^{atm} based on $\Delta\delta^{13}C$ could be valid for a wide range of (bio)geochemical states. Locally however, $\Delta\delta^{13}C$ can respond differently to (bio)geochemical processes, as shown in this study. pCO_2^{atm}, $\delta^{13}C^{atm}$ and marine $\delta^{13}C$ are shown to be disproportionally sensitive to SO gas exchange rate changes, with lower latitudes offsetting part of this sensitivity. The effect of the sea ice cover on pCO_2^{atm} and $\delta^{13}C^{atm}$ as well as marine $\delta^{13}C$ depends strongly on the location of the sea ice edge, but has strong potential to change any of them. The experiments on POC sinking rate and SO nutrient uptake show that their effect on pCO_2^{atm} is different from the effect on $\delta^{13}C^{atm}$. $\delta^{13}C^{atm}$ is dominated by the loss of light carbon in the POC sinking rate experiment, while the reduction of SO carbon outgassing dominates the sensitivity to the V_{max} experiment. In the Vmax experiment $\Delta\delta^{13}C$ strengthens in the SO but not in other regions, while in the global increased POC sinking rate experiment $\Delta\delta^{13}C$ is not very sensitive in the SO but strengthens in low latitudes.

Mean $\Delta\delta^{13}C$ in our experiments (assuming a constant ocean circulation) varies no more than 0.5 ‰ due to (bio)geochemical state changes (Fig. 4). This amplitude is about half of the reconstructed variation in $\Delta\delta^{13}C$ on glacial-interglacial timescales, and could thus contribute to variation in $\Delta\delta^{13}C$ together with water column stratification. Locally, $\Delta\delta^{13}C$ variations can surpass or mirror the 0.5 ‰ constraint however, due to the spatial variation in the sensitivity of $\delta^{13}C$ to biogeochemical change. This emphasises the importance of constraining the (bio)geochemical environment before interpreting $\Delta\delta^{13}C$ from sediment cores.

The variations in $\Delta\delta^{13}C$ are caused by both biology and gas exchange processes in the surface ocean but mostly by biological processes in the deep ocean. The role of the SO in $\Delta\delta^{13}C$ variations is likely to be disproportionally large, as based on the sensitivity of the global $\delta^{13}C$ distribution and mean $\Delta\delta^{13}C$ to SO-only (bio)geochemical change (i.e. SO-only experiment for gas exchange, the V_{max} experiment and the sea ice experiments).

As an outlook, the use of a more complex model with more ecosystem variables (i.e. more trophic levels), a higher horizontal and vertical resolution and a shorter time-step (resolving seasonal variations) could provide valuable additional information. For example, the role of different regions within the SO on the global $\delta^{13}C$ distribution could be better studied with a more complex model. Sediment core-based reconstructions of the global carbon cycle could possibly be aided by a more complex model with a finer grid and higher time resolution, by providing more detailed information on the contribution of

(bio)geochemical processes to local ocean tracers. Next to that, exploring the effect on $\Delta\delta^{13}C$ of a glacial model circulation field could provide a way to quantify the maximum combined effect of circulation and (bio)geochemical change on $\Delta\delta^{13}C$.

Acknowledgements. This study is a contribution to the project "Earth system modelling of climate variations in the Anthropocene" (EVA; grant no. 229771) as well as the project "Overturning circulation and its implications for global carbon cycle in coupled models" (ORGANIC; grant no. 239965) which are both funded by the Research Council of Norway. This is a contribution to the Bjerknes Centre for Climate Research (Bergen, Norway). Storage resources were provided by the Norwegian storage infrastructure of Sigma2 (NorStore project ns2980k).

References

Bauska, T. K., Baggenstos, D., Brook, E. J., Mix, A. C., Marcott, S. A., Petrenko, V. V., Schaefer, H., Severinghaus, J. P., and Lee, J. E.: Carbon isotopes characterize rapid changes in atmospheric carbon dioxide during the last deglaciation, P Natl Acad Sci USA, 113, 3465-3470, 10.1073/pnas.1513868113, 2016.

Broecker, W. S., and Maier-Reimer, E.: The influence of air and sea exchange on the carbon isotope distribution in the sea, Global Biogeochemical Cycles, 6, 315-320, 10.1029/92GB01672, 1992.

Broecker, W. S., and McGee, D.: The 13C record for atmospheric CO2: What is it trying to tell us?, Earth and Planetary Science Letters, 368, 175-182, http://dx.doi.org/10.1016/j.epsl.2013.02.029, 2013.

Charles, C. D., Pahnke, K., Zahn, R., Mortyn, P. G., Ninnemann, U., and Hodell, D. A.: Millennial scale evolution of the Southern Ocean chemical divide, Quaternary Science Reviews, 29, 399-409, 10.1016/j.quascirev.2009.09.021, 2010.

Crosta, X.: Antarctic Sea Ice History, Late Quaternary, in: Encyclopedia of Paleoclimatology and Ancient Environments, edited by: Gornitz, V., Springer Netherlands, Dordrecht, 31-34, 2009.

Crucifix, M.: Distribution of carbon isotopes in the glacial ocean: A model study, Paleoceanography, 20, n/a-n/a, 10.1029/2005PA001131, 2005.

Curry, W. B., and Oppo, D. W.: Glacial water mass geometry and the distribution of δ13C of ΣCO2 in the western Atlantic Ocean, Paleoceanography, 20, n/a-n/a, 10.1029/2004PA001021, 2005.

DeVries, T., Primeau, F., and Deutsch, C.: The sequestration efficiency of the biological pump, Geophysical Research Letters, 39, L13601, 10.1029/2012GL051963, 2012.

Dickson, A. J., Leng, M. J., and Maslin, M. A.: Mid-depth South Atlantic Ocean circulation and chemical stratification during MIS-10 to 12: implications for atmospheric CO₂, Clim. Past, 4, 333-344, 10.5194/cp-4-333-2008, 2008.

Dunne, J. P., Sarmiento, J. L., and Gnanadesikan, A.: A synthesis of global particle export from the surface ocean and cycling through the ocean interior and on the seafloor, Global Biogeochemical Cycles, 21, GB4006, 10.1029/2006GB002907, 2007.

Eide, M., Olsen, A., Ninnemann, U. S., and Eldevik, T.: A global estimate of the full oceanic 13C Suess effect since the preindustrial, Global Biogeochemical Cycles, 31, 492-514, 10.1002/2016GB005472, 2017a.

Eide, M., Olsen, A., Ninnemann, U. S., and Johannessen, T.: A global ocean climatology of preindustrial and modern ocean δ13C, Global Biogeochemical Cycles, 31, 515-534, 10.1002/2016GB005473, 2017b.

Emerson, S., and Hedges, J.: Chemical oceanography and the marine carbon cycle, Cambridge University Press, Cambridge, xi, 453 p. 458 p. of col. plates pp., 2008.

Galbraith, E. D., Kwon, E. Y., Bianchi, D., Hain, M. P., and Sarmiento, J. L.: The impact of atmospheric pCO2 on carbon isotope ratios of the atmosphere and ocean, Global Biogeochemical Cycles, 29, 307-324, 10.1002/2014GB004929, 2015.

Gottschalk, J., Skinner, L. C., Lippold, J., Vogel, H., Frank, N., Jaccard, S. L., and Waelbroeck, C.: Biological and physical controls in the Southern Ocean on past millennial-scale atmospheric CO2 changes, 7, 11539, 10.1038/ncomms11539 https://www.nature.com/articles/ncomms11539#supplementary-information, 2016.

Gruber, N., and Keeling, C. D.: An improved estimate of the isotopic air-sea disequilibrium of CO2: Implications for the oceanic uptake of anthropogenic CO2, Geophysical Research Letters, 28, 555-558, 10.1029/2000GL011853, 2001.

Heinze, C., Maier-Reimer, E., and Winn, K.: Glacial pCO2 Reduction by the World Ocean: Experiments With the Hamburg Carbon Cycle Model, Paleoceanography, 6, 395-430, 10.1029/91PA00489, 1991.

Heinze, C., and Hasselmann, K.: Inverse Multiparameter Modeling of Paleoclimate Carbon Cycle Indices, Quaternary Research, 40, 281-296, https://doi.org/10.1006/qres.1993.1082, 1993.

Heinze, C., Maier-Reimer, E., Winguth, A. M. E., and Archer, D.: A global oceanic sediment model for long-term climate studies, Global Biogeochemical Cycles, 13, 221-250, 10.1029/98GB02812, 1999.

Heinze, C.: Assessing the importance of the Southern Ocean for natural atmospheric pCO2 variations with a global biogeochemical general circulation model, Deep Sea Research Part II: Topical Studies in Oceanography, 49, 3105-3125, http://dx.doi.org/10.1016/S0967-0645(02)00074-7, 2002.

Heinze, C., Hoogakker, B. A. A., and Winguth, A.: Ocean carbon cycling during the past 130 000 years – a pilot study on inverse palaeoclimate record modelling, Clim. Past, 12, 1949-1978, 10.5194/cp-12-1949-2016, 2016.

Hilting, A. K., Kump, L. R., and Bralower, T. J.: Variations in the oceanic vertical carbon isotope gradient and their implications for the Paleocene-Eocene biological pump, Paleoceanography, 23, n/a-n/a, 10.1029/2007PA001458, 2008.

Holden, P. B., Edwards, N. R., Müller, S. A., Oliver, K. I. C., Death, R. M., and Ridgwell, A.: Controls on the spatial distribution of oceanic δ13C_DIC, Biogeosciences, 10, 1815-1833, 10.5194/bg-10-1815-2013, 2013.

Hollander, D. J., and McKenzie, J. A.: CO2 control on carbon-isotope fractionation during aqueous photosynthesis: A paleo-pCO2 barometer, Geology, 19, 929-932, 10.1130/0091-7613(1991)019<0929:ccocif>2.3.co;2, 1991.

Hoogakker, B. A. A., Elderfield, H., Schmiedl, G., McCave, I. N., and Rickaby, R. E. M.: Glacial-interglacial changes in bottom-water oxygen content on the Portuguese margin, Nature Geosci, 8, 40-43, 10.1038/ngeo2317 http://www.nature.com/ngeo/journal/v8/n1/abs/ngeo2317.html#supplementary-information, 2015.

Jahn, A., Lindsay, K., Giraud, X., Gruber, N., Otto-Bliesner, B. L., Liu, Z., and Brady, E. C.: Carbon isotopes in the ocean model of the Community Earth System Model (CESM1), Geoscientific Model Development, 8, 2419-2434, 10.5194/gmd-8-2419-2015, 2015.

Jansen, M. F.: Glacial ocean circulation and stratification explained by reduced atmospheric temperature, Proceedings of the National Academy of Sciences, 114, 45-50, 10.1073/pnas.1610438113, 2017.

Jones, D. C., Ito, T., Takano, Y., and Hsu, W.-C.: Spatial and seasonal variability of the air-sea equilibration timescale of carbon dioxide, Global Biogeochemical Cycles, 28, 1163-1178, 10.1002/2014GB004813, 2014.

Kroopnick, P.: The distribution of 13C in the Atlantic Ocean, Earth and Planetary Science Letters, 49, 469-484, https://doi.org/10.1016/0012-821X(80)90088-6, 1980.

Kroopnick, P. M.: The distribution of 13C of ΣCO2 in the world oceans, Deep Sea Research Part A. Oceanographic Research Papers, 32, 57-84, https://doi.org/10.1016/0198-0149(85)90017-2, 1985.

Laws, E. A., Bidigare, R., R., and Popp, B. N.: Effects of growth rate and CO2 concentration on carbon isotopic fractionation by the marine diatom Phaeodactylum tricornutum, Limnol. Oceanogr., 42, 1552-1560, 1997.

Lutz, M. J., Caldeira, K., Dunbar, R. B., and Behrenfeld, M. J.: Seasonal rhythms of net primary production and particulate organic carbon flux to depth describe the efficiency of biological pump in the global ocean, Journal of Geophysical Research: Oceans, 112, C10011, 10.1029/2006JC003706, 2007.

Lynch-Stieglitz, J., Stocker, T. F., Broecker, W. S., and Fairbanks, R. G.: The influence of air-sea exchange on the isotopic composition of oceanic carbon: Observations and modeling, Global Biogeochemical Cycles, 9, 653-665, 10.1029/95GB02574, 1995.

MacCready, P., and Quay, P.: Biological export flux in the Southern Ocean estimated from a climatological nitrate budget, Deep Sea Research Part II: Topical Studies in Oceanography, 48, 4299-4322, http://dx.doi.org/10.1016/S0967-0645(01)00090-X, 2001.

Mackenzie, F. T., and Lerman, A.: Isotopic Fractionation of Carbon: Inorganic and Biological Processes, in: Carbon in the Geobiosphere — Earth's Outer Shell —, edited by: Mackenzie, F. T., and Lerman, A., Springer Netherlands, Dordrecht, 165-191, 2006.

Marchal, O., Stocker, T. F., and Joos, F.: A latitude-depth, circulation-biogeochemical ocean model for paleoclimate studies. Development and sensitivities, Tellus B, 50, 290-316, 10.1034/j.1600-0889.1998.t01-2-00006.x, 1998.

Marinov, I., Gnanadesikan, A., Toggweiler, J. R., and Sarmiento, J. L.: The Southern Ocean biogeochemical divide, Nature, 441, 964-967, http://www.nature.com/nature/journal/v441/n7096/suppinfo/nature04883.html, 2006.

Mook, W. G.: 13C in atmospheric CO2, Netherlands Journal of Sea Research, 20, 211-223, http://dx.doi.org/10.1016/0077-7579(86)90043-8, 1986.
Nevison, C. D., Keeling, R. F., Kahru, M., Manizza, M., Mitchell, B. G., and Cassar, N.: Estimating net community production in the Southern Ocean based on atmospheric potential oxygen and satellite ocean color data, Global Biogeochemical Cycles, 26, GB1020, 10.1029/2011GB004040, 2012.
Oliver, K. I. C., Hoogakker, B. A. A., Crowhurst, S., Henderson, G. M., Rickaby, R. E. M., Edwards, N. R., and Elderfield, H.: A synthesis of marine sediment core δ13C data over the last 150 000 years, Climate of the Past, 6, 645-673, 2010.
Primeau, F. W., Holzer, M., and DeVries, T.: Southern Ocean nutrient trapping and the efficiency of the biological pump, Journal of Geophysical Research: Oceans, 118, 2547-2564, 10.1002/jgrc.20181, 2013.
Quay, P., Sonnerup, R., Westby, T., Stutsman, J., and McNichol, A.: Changes in the 13C/12C of dissolved inorganic carbon in the ocean as a tracer of anthropogenic CO2 uptake, Global Biogeochemical Cycles, 17, 4-1-4-20, 10.1029/2001GB001817, 2003.
Sarmiento, J. L., Gruber, N., Brzezinski, M. A., and Dunne, J. P.: High-latitude controls of thermocline nutrients and low latitude biological productivity, Nature, 427, 56-60, 2004.
Schlitzer, R.: Carbon Export Fluxes in the Southern Ocean: Results from Inverse Modeling and Comparison with Satellite Estimates, Deep Sea Research, 2, 1623-1644, 2002.
Schmittner, A., Gruber, N., Mix, A. C., Key, R. M., Tagliabue, A., and Westberry, T. K.: Biology and air-sea gas exchange controls on the distribution of carbon isotope ratios (δ13C) in the ocean, Biogeosciences, 10, 5793-5816, 10.5194/bg-10-5793-2013, 2013.
Shackleton, N. J., and Pisias, N. G.: Atmospheric carbon dioxide, orbital forcing, and climate, in: The Carbon cycle and atmospheric CO2: natural variations archean to present, edited by: Sundquist, E. T., and Broecker, W. S., Geophysical Monograph, American Geophysical Union, Washington, 303-317, 1985.
Sonnerup, R. E., and Quay, P. D.: 13C constraints on ocean carbon cycle models, Global Biogeochemical Cycles, 26, GB2014, 10.1029/2010GB003980, 2012.
Stenström, K. E., Skog, G., Georgiadou, E., Genberg, J., and Johansson, A.: A guide to radiocarbon units and calculations, Lund University, Lund, 18, 2011.
Stephens, B. B., and Keeling, R. F.: The influence of Antarctic sea ice on glacial–interglacial CO 2 variations, Nature, 404, 171, 10.1038/35004556, 2000.
Stuiver, M., and Pollack, H. A.: Reporting of C-14 data—Discussion, 363-365 pp., 1977.
Tagliabue, A., and Bopp, L.: Towards understanding global variability in ocean carbon-13, Global Biogeochemical Cycles, 22, GB1025, 10.1029/2007GB003037, 2008.
Zahn, R., Winn, K., and Sarnthein, M.: Benthic foraminiferal δ13C and accumulation rates of organic carbon: Uvigerina Peregrina group and Cibicidoides Wuellerstorfi, Paleoceanography, 1, 27-42, 10.1029/PA001i001p00027, 1986.
Zeebe, R., and Wolf-Gladrow, D.: CO2 in Seawater: Equilibrium, Kinetics, Isotopes, Elsevier Oceanography Series, edited by: Halpern, D., Elsevier Science B.V., Amsterdam, The Netherlands, 346 pp., 2001.
Zhang, J., Quay, P. D., and Wilbur, D. O.: Carbon isotope fractionation during gas-water exchange and dissolution of CO2, Geochimica et Cosmochimica Acta, 59, 107-114, http://dx.doi.org/10.1016/0016-7037(95)91550-D, 1995.
Ziegler, M., Diz, P., Hall, I. R., and Zahn, R.: Millennial-scale changes in atmospheric CO2 levels linked to the Southern Ocean carbon isotope gradient and dust flux, Nature Geosci, 6, 457-461, 10.1038/ngeo1782
http://www.nature.com/ngeo/journal/v6/n6/abs/ngeo1782.html#supplementary-information, 2013.

Biogeosciences Discuss., https://doi.org/10.5194/bg-2018-52
Manuscript under review for journal Biogeosciences
Discussion started: 26 February 2018

Experiment	Experiment setup
Gas fast	CO_2 gas exchange rate * 4
Gas slow	CO_2 gas exchange rate / 4
Efficient biological pump	POC sinking rate doubled to 6m/d
Inefficient biological pump	POC sinking rate halved to 1.5m/d
V_{max}	High nutrient uptake rate (control*50) in the Southern Ocean
Ice large	Southern Ocean sea ice cover south of 50° S
Ice small	Southern Ocean sea ice cover south of 70° S

Table 1 Description of the sensitivity experiments. The sensitivity experiments on the CO_2 gas exchange rate and the biological pump have been done twice, once for the Global Ocean and once only making changes in the Southern Ocean (south of 45° S).

Biogeosciences Discuss., https://doi.org/10.5194/bg-2018-52
Manuscript under review for journal Biogeosciences
Discussion started: 26 February 2018

	Global experiments		SO-only experiments	
	pCO_2^{atm}	$\delta^{13}C^{atm}$	pCO_2^{atm}	$\delta^{13}C^{atm}$
Control	279	-6,4	-	
Gas exchange				
Fast	288	-6,8	284	-6,9
Slow	284	-6,3	281	-6,1
Biological pump				
POC: Efficient	252	-6,2	275	-6,4
POC: Inefficient	293	-6,7	283	-6,5
V_{max}	-		251	-6,6
Ice				
Large	-		284	-6,1
Small	-		274	-6,6

Table 2 Results of pCO_2^{atm} [ppm] and $\delta^{13}C^{atm}$ [‰] for all sensitivity experiments.

Biogeosciences Discuss., https://doi.org/10.5194/bg-2018-52
Manuscript under review for journal Biogeosciences
Discussion started: 26 February 2018

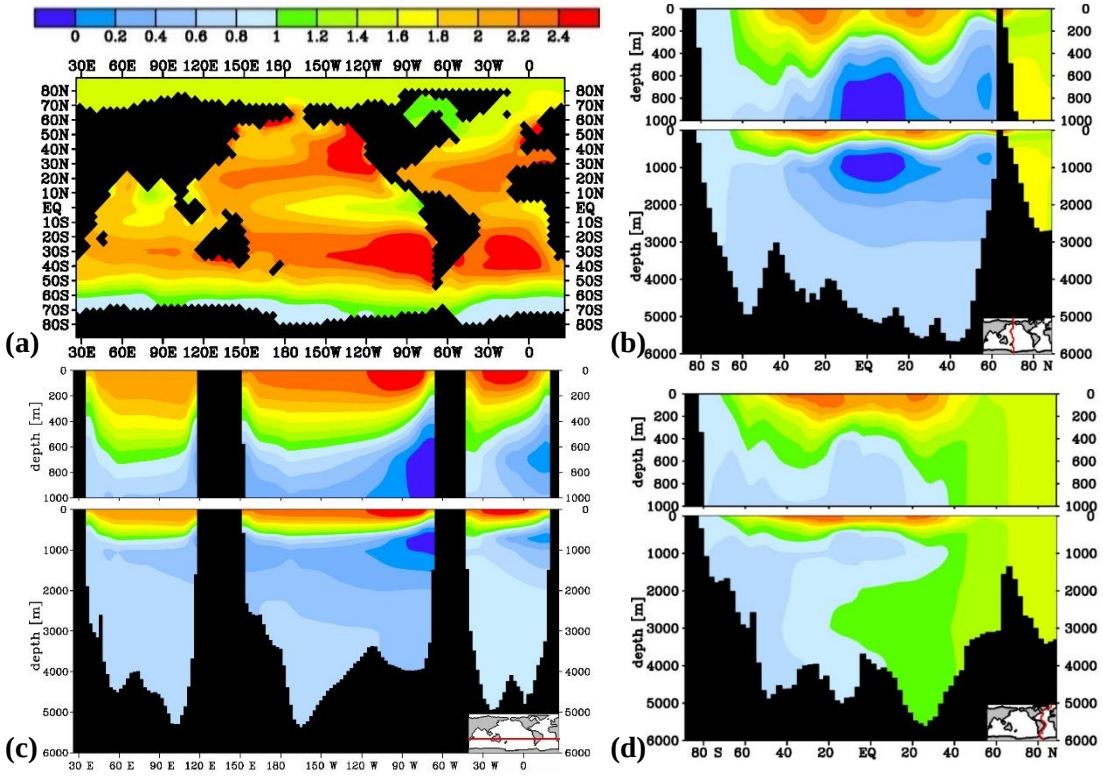

Figure 1 Modelled $\delta^{13}C$ of DIC [‰] distribution for the model control run: (a) $\delta^{13}C$ at 25 m depth, (b) Pacific transect of $\delta^{13}C$, (c) Zonal transect of $\delta^{13}C$ at 26° S, and (d) Atlantic transect of $\delta^{13}C$.

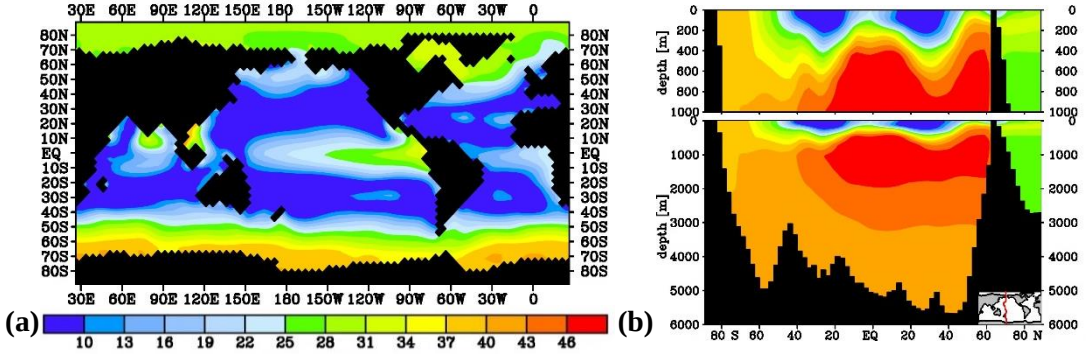

Figure 2 $\delta^{13}C_{bio}^{perc}$, the contribution of biology to the local $\delta^{13}C$ signal [%], as calculated using Eq. (3) at (a) 25 m depth and (b) a Pacific transect. The remainder of 100 % is attributed to air-sea gas exchange. The $\delta^{13}C$bio and $\delta^{13}C_{AS}$ values in ‰ are very similar to the values found by Schmittner et al. (2013).

Biogeosciences Discuss., https://doi.org/10.5194/bg-2018-52
Manuscript under review for journal Biogeosciences
Discussion started: 26 February 2018

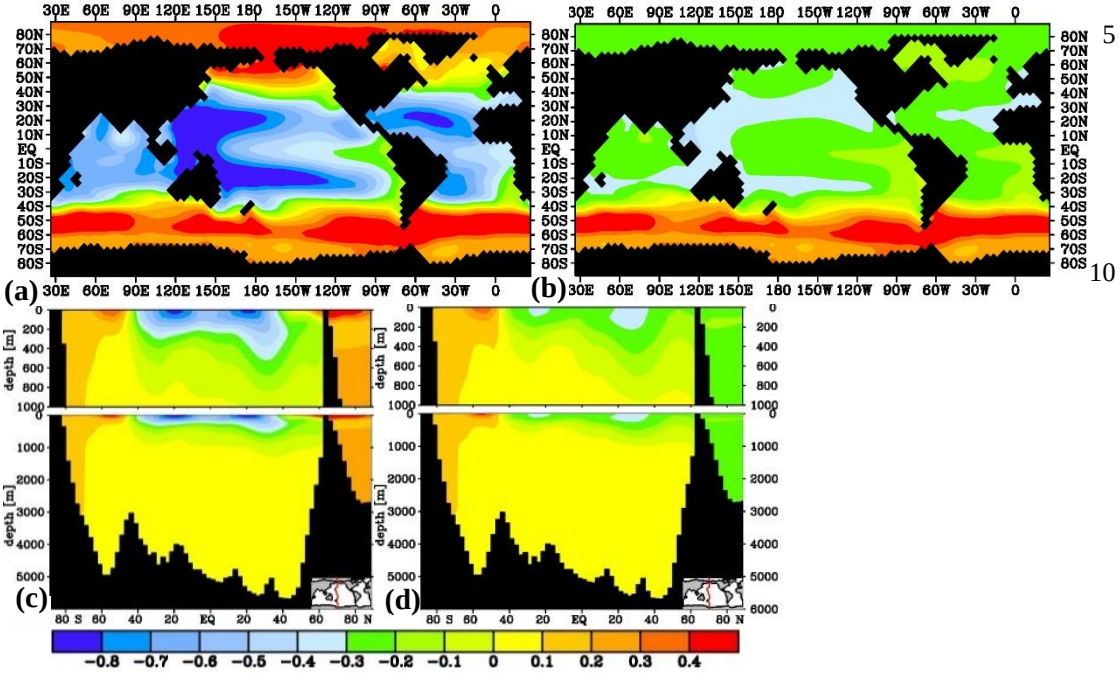

Figure 3 Modelled fast gas exchange sensitivity experiment $\delta^{13}C$ of DIC [‰] difference with the model control run: global experiments (a) and (c) and SO-only experiments (b) and (d), at 25 m depth (a) and (b) and as a Pacific transect of $\delta^{13}C$ difference (c) and (d).

Biogeosciences Discuss., https://doi.org/10.5194/bg-2018-52
Manuscript under review for journal Biogeosciences
Discussion started: 26 February 2018

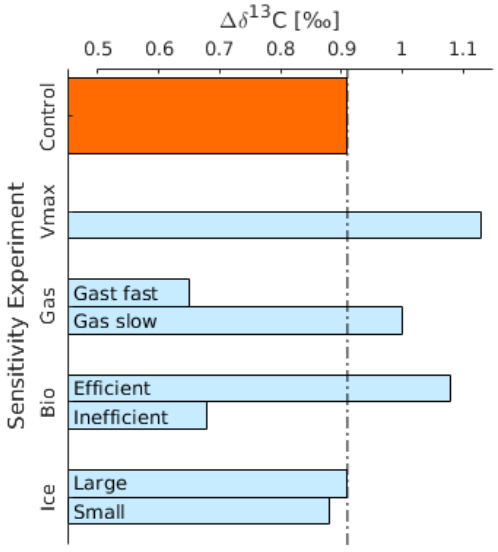

Figure 4 Global mean $\Delta\delta^{13}C$ for the different sensitivity experiments. The results for the Southern Ocean only experiments (Sect. 2) are described in the text.

Biogeosciences Discuss., https://doi.org/10.5194/bg-2018-52
Manuscript under review for journal Biogeosciences
Discussion started: 26 February 2018

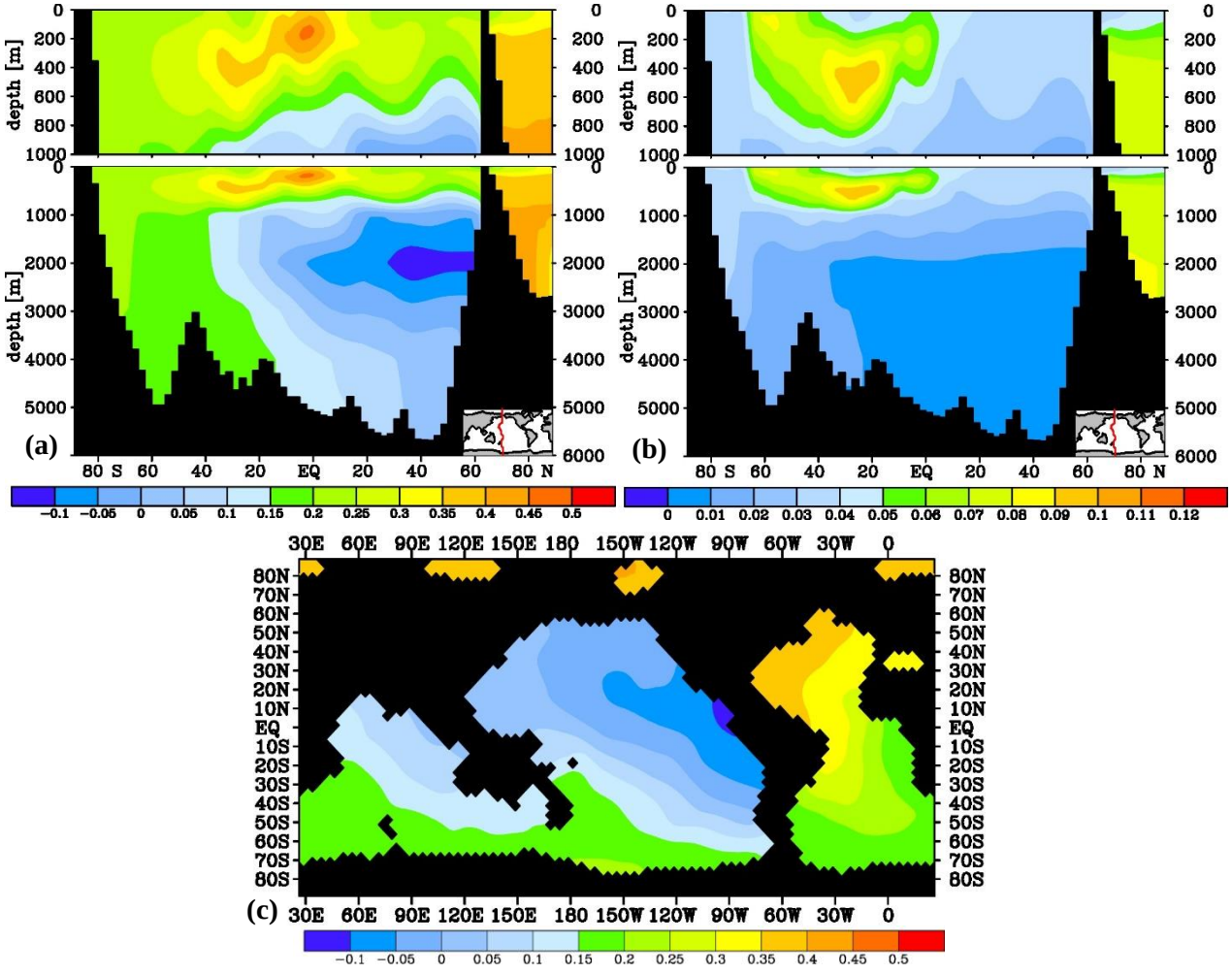

Figure 5 $\delta^{13}C$ of DIC difference between model control run and (a) the global efficient biological pump (high POC sinking rate) experiment for a Pacific transect and (b) the SO-only efficient biological pump (high POC sinking rate) experiment for a Pacific transect and (c) at 3000m depth for the global efficient biological pump experiment. Note the different scales.

Biogeosciences Discuss., https://doi.org/10.5194/bg-2018-52
Manuscript under review for journal Biogeosciences
Discussion started: 26 February 2018

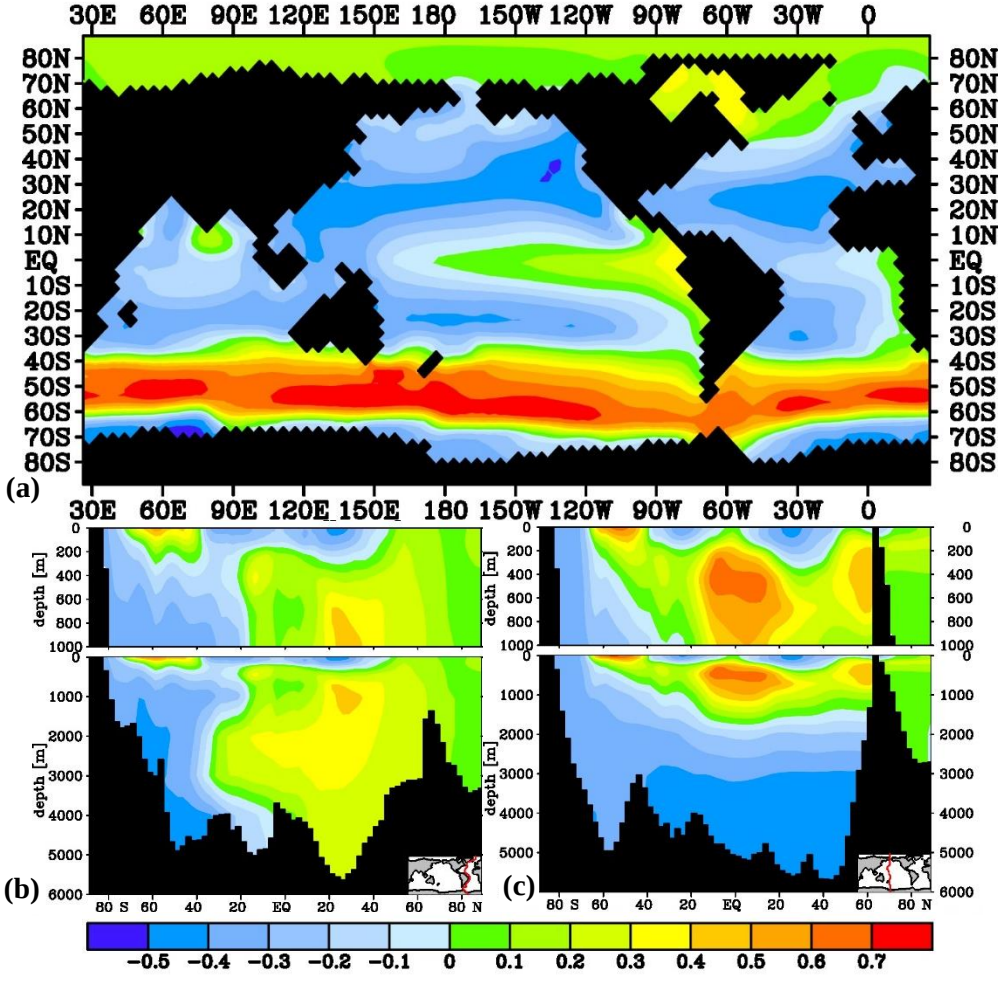

Figure 6 Difference plots between the model control run and the V_{max} nutrient depletion experiment at (a) 25m depth and for (b) an Atlantic transect and (c) a Pacific transect.

Biogeosciences Discuss., https://doi.org/10.5194/bg-2018-52
Manuscript under review for journal Biogeosciences
Discussion started: 26 February 2018

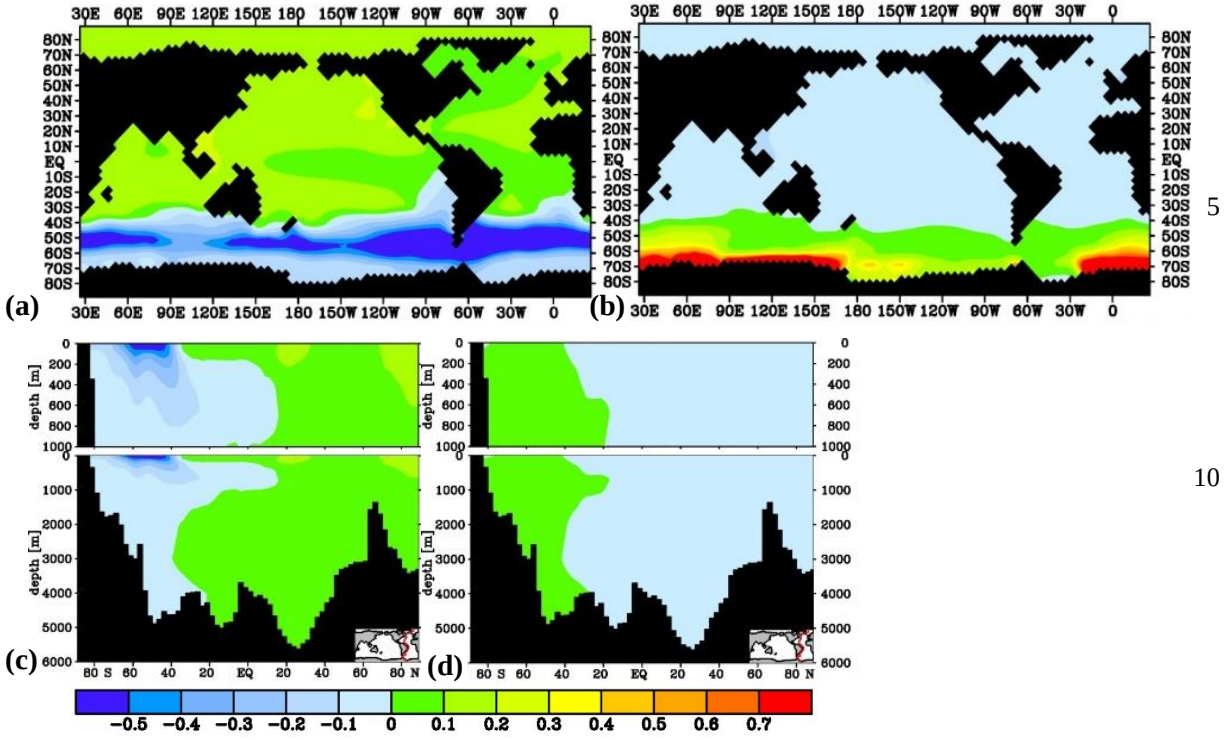

Figure 7 The effect of a large (a, c) and small (b, d) Antarctic sea ice cover on $\delta^{13}C$ as compared to the control for 25 m depth (a, b) and an Atlantic transect (c, d).

Biogeosciences Discuss., https://doi.org/10.5194/bg-2018-52
Manuscript under review for journal Biogeosciences
Discussion started: 26 February 2018

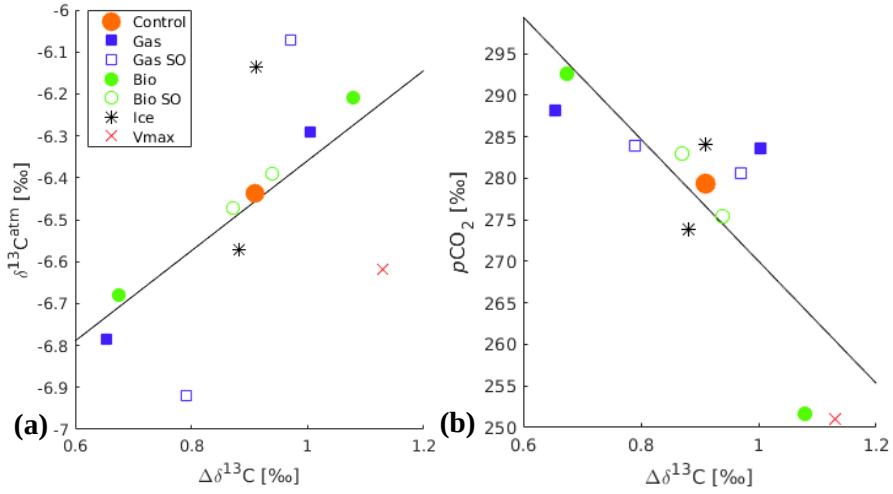

Figure 8 Scatter plot of the mean $\Delta\delta^{13}C$ and (a) $\delta^{13}C^{atm}$ of the different sensitivity experiments. R-squared of the best-fit line is 0.345 (p-value 0.0445), and the line is described by y=1.1x-7.4 (b) pCO_2^{atm} of the different sensitivity experiments. R-squared of the best-fit line is 0.645 (p-value 0.00166), and the line is described by y=-74x+344.